doi:10.1093/brain/awl392 *Brain* (2007), **130**, 995–1008

Peri-infarct depolarizations lead to loss of perfusion in ischaemic gyrencephalic cerebral cortex

Anthony J. Strong,[1] Peter J. Anderson,[1] Helena R. Watts,[1] David J. Virley,[2] Andrew Lloyd,[2] Elaine A. Irving,[2] Toshiaki Nagafuji,[2] Mitsuyoshi Ninomiya,[2] Hajime Nakamura,[4] Andrew K. Dunn[3] and Rudolf Graf[4]

[1]King's College London, Department of Clinical Neurosciences (Neurosurgery), UK, [2]Shionogi-GlaxoSmithKline LLC, [3]University of Texas at Austin, Biomedical Engineering, Austin, TX, USA and [4]Max-Planck Institute for Neurological Research, Cologne, Germany

Correspondence to: Prof. Anthony J. Strong, Department of Neurosurgery, King's College Hospital, London SE5 9RS, UK
E-mail: anthony.strong@kcl.ac.uk

In the light of accumulating evidence for the occurrence of spontaneous cortical spreading depression and peri-infarct depolarizations in the human brain injured by trauma or aneurysmal subarachnoid haemorrhage, we used DC electrode recording and laser speckle imaging to study the relationship between depolarization events and perfusion in the ischaemic, gyrencephalic brain. In 14 adult male cats anaesthetized with chloralose, one cerebral hemisphere was exposed and the middle cerebral artery occluded. Surface cortical perfusion in core and penumbral territories was imaged semiquantitatively at intervals of 13 s for 4 h. Cortical surface DC potential was recorded. Time interval between changes in DC potential and in perfusion was examined, and this comparison was repeated using microelectrodes for DC potential in five similar experiments in a second laboratory. Mean pre-occlusion perfusion was 11707 ± 4581 units (equivalent to CBF (cerebral blood flow) ~40.5 ± SD 14.4 ml/100 g/min), and fell on occlusion to 5318 ± 2916 (CBF ~17.1 ± 8.3), 5291 ± 3407 (CBF ~17.0 ± 10.1), and 6711 ± 3271 (CBF ~22.2 ± 9.6), quickly recovering to 8704 ± 4581 (CBF ~29.5 ± 14.4), 9741 ± 4499 (CBF ~33.3 ± 14.1) and 10 314 ± 3762 (CBF ~35.4 ± 11.4) on the core, intermediate and outer penumbral gyri, respectively. Mean perfusion later fell secondarily on core and intermediate gyri but, overall, was preserved on the outer (upper level of perfusion) gyrus during the period of observation. Pattern and severity of transient changes in perfusion associated with depolarization events varied with gyral location; falls in perfusion were sometimes profound and irreversible, and followed rather than preceded depolarization. In this model of occlusive stroke, reductions in perfusion linked to peri-infarct depolarization events contribute to secondary deterioration in penumbral areas. The findings suggest that such events play a central rather than a subsidiary role in cerebral infarction in the gyrencephalic brain.

Keywords: penumbra; depolarization; spreading cortical depression; laser speckle imaging; middle cerebral artery occlusion

Abbreviations: CSD = cortical spreading depression; CBF = cerebral blood flow; ECoG = electrocorticographic; EG = ectosylviangyrus; MAP = mean arterial pressure; MCAO = middle cerebral artery occlusion; MG = marginalgyrus; PIDs = peri-infarct depolarizations; SAH = subarachnoid haemorrhage; SG = suprasylviangyrus

Received June 22, 2006. Revised November 15, 2006 and December 18, 2006. Accepted December 22, 2006

Introduction

The development of a phase of delayed neurological deterioration several days after first symptoms of an ictal cerebrovascular event such as major, occlusive stroke or aneurysmal subarachnoid haemorrhage (SAH) is often associated with worse outcome, is not well understood, and is difficult to treat. Recently, a group of publications have reported the occurrence of spontaneous, recurrent episodes of transient or more protracted depression of electrocorticographic (ECoG) activity propagating across the cortex in patients with contusional head injury (Strong *et al.*, 2002) or aneurysmal SAH (Dreier *et al.*, 2006); it has been shown that such episodes closely resemble the transient cortical depolarization which is characteristic of spreading cortical depression of Leão (Leao, 1944*b*; Fabricius *et al.*, 2006). These new findings focus attention on the cerebral microcirculation, suggesting the possibility of a process in which depolarization and deterioration in perfusion might be linked; however, the sequence of

causality remains unclear. The potential contribution of disturbed vascular mechanisms to deterioration has recently been further supported by a body of experimental work that requires brief review.

In his original demonstration in the rabbit brain of cortical spreading depression (CSD), which required to be 'induced' by local stimulation, Leão showed that the depolarization event propagated throughout the cortical field that he studied; this comprised most of the convexity of the ipsilateral hemisphere (Leao, 1944*b*). He also described hyperaemia associated with CSD (Leao, 1944*a*). Such 'normal', hyperaemic (the initial phase of the perfusion response) CSD is not damaging (Nedergaard and Hansen, 1988). In contrast, 'spontaneous', transient increases in extracellular potassium ion concentration occurring in cerebral cortex lying within the ischaemic penumbra were first described following middle cerebral artery occlusion (MCAO) in baboons (Branston *et al.*, 1977) and in cats (Strong *et al.*, 1983). Their properties and effects have been elucidated in extensive work by many research groups, and their designation as peri-infarct depolarizations (PIDs) has been widely adopted (Hossmann, 1996). More recently, the capacity of PIDs to propagate widely in the penumbra in the ischaemic, gyrencephalic brain has been demonstrated directly by serial imaging of spread, as marked by an increase in endogenous cortical fluorescence (Strong *et al.*, 1996). Peri-infarct depolarizations enlarge infarct size: Mies and his colleagues demonstrated a linear relationship between infarct size and number of spontaneous PIDs (Mies *et al.*, 1993), and it was later shown, critically, that number of PIDs is the determining variable in this relationship (Back *et al.*, 1996; Busch *et al.*, 1996; Takano *et al.*, 1996). Dijkhuisen and colleagues proposed that the total duration of depolarizations may be more predictive of the size of the definitive lesion than is their number (Dijkhuizen *et al.*, 1999).

Since then, a number of original reports of studies of SAH in rats (Dreier *et al.*, 1998, 2000, 2002*b*) and of focal ischaemia in mice (Shin *et al.*, 2006) have suggested that in these models spreading depolarizations are associated with reductions in perfusion rather than with the hyperaemia typical of CSD in the normally perfused brain as first shown by Leão; similar findings in cats subject to MCAO were reported in abstract form by Strong *et al.* (2003). These findings, taken together with the new results in patients with SAH from Dreier *et al.* (2006), indicate a clear need for more detailed information on the relationship of depolarization events with changes in perfusion in the ischaemic 'gyrencephalic' brain. Studies in the gyrencephalic brain are required because of the recognized role of astrocytes in extracellular glutamate and potassium homeostasis, increasing support for the role of astrocytes and their foot processes in neurovascular coupling (Takano *et al.*, 2006), the considerably higher ratio of astrocytes to neurons in the human than in the rodent brain (Tower and Young, 1973), the greater complexity of astrocytes in the human brain (Oberheim *et al.*, 2006), and evidence that PIDs are less frequent in the gyrencephalic than in the rodent brain (Strong *et al.*, 2000) [together with the negative results of many clinical neuroprotection studies largely based on experimental findings in rodent models (Narayan *et al.*, 2002)].

The unpredictable spatial and temporal pattern of PID occurrence and propagation in MCAO models has made it difficult to probe vasoreactivity to PIDs in detail with methods for assessing cortical perfusion such as laser Doppler flow monitoring; such methods probe only single cortical foci and cannot assess the territory as a whole. To examine the relationship of PIDs with changes in perfusion in the widest possible area of penumbra in the gyrencephalic brain, we applied instead laser speckle flowmetry in the present (non-recovery) experiments in cats in Laboratory 1 (King's College London), to collect sequential images of perfusion over a large portion of the penumbral territory continuously for 4 h after permanent MCAO. A further goal of the experiments was to describe the time course(s) of changes in perfusion at defined cortical sites during depolarization events, so as to provide one or more 'time-series signatures' that might later be sought from continuous monitoring of perfusion with techniques now available clinically for patients undergoing neurosurgery (Vajkoczy *et al.*, 2000). We monitored cortical surface DC potential as a reference method for detection of PIDs. In several experiments we observed striking, stepwise reductions in perfusion that occurred at delayed intervals after MCAO and propagated in the penumbra: these were closely linked with DC potential transients characteristic of PIDs, and invariably 'followed' the change in DC potential. This important temporal sequence was subsequently confirmed with microelectrodes in a second laboratory (Cologne). The studies in Laboratory 1 were conducted in the vehicle-treated group for a neuroprotection study that will be reported separately.

Material and methods

Anaesthesia and surgical preparation

The important feature of the anaesthesia used in both laboratories was the use of α-chloralose during experimental data collection and imaging (with only minimal temporary supplementation with 0.5–1% inhaled halogen if any increase in blood pressure required this). The purpose of this was to minimize pharmacological suppression of spontaneous depolarizations, an effect of halogens demonstrated by Saito *et al.* (1995).

Laboratory 1 (London)

In experiments carried out in full compliance with UK legislation (PPL 70-5894), anaesthesia was induced with medetomidine hydrochloride 0.1 mg/kg and 4% isofluorane in 14 adult male cats in the weight range 3.3–5.2 kg. Femoral arterial and venous catheters were inserted for serial measurement of arterial pressure and blood gases, and for administration of drugs, respectively.

The trachea was intubated and artificial ventilation established, maintained and adjusted as required, with a target value of arterial pCO_2 of 30 mmHg. Sodium chloride 0.9% buffered with bicarbonate to pH 7.4 was infused intravenously at 4 ml/kg/h throughout surgery and subsequent observation/imaging for 4 h after MCAO. Any metabolic acidosis was corrected by small intravenous bolus doses of 8.3% sodium bicarbonate.

When mean arterial pressure (MAP) had stabilized within the range 80–100 mmHg, α-chloralose 60 mg/kg (Sigma-Aldrich UK) at 60°C was infused intravenously over 5 min, and inspired isofluorane concentration reduced and maintained/adjusted at the minimum compatible with the target MAP range; this concentration was typically 0–1.0%. The right middle cerebral artery was exposed transorbitally in all experiments and occluded after baseline data acquisition with a miniature Scoville clip. The scalp and calvarium were removed and the dura opened over the right cerebral hemisphere so as to expose a part of the ectosylvian (EG), and most of the suprasylvian (SG) and marginal (MG) gyri (thus concentrating on penumbra, Fig. 1A), and a pool established and filled with mineral oil; a water-heated coil was inserted into the pool and the pool temperature monitored and maintained at 37 ± 0.5°C. Occasional instances of later increase in MAP were managed by temporary minimal increase in inspired isofluorane concentration of up to 1%, substituted if necessary by additional infusions of α-chloralose 30 mg/kg at 30-min intervals until MAP returned within original levels.

Laboratory 2 (Koeln)

The study was approved by the local animal care committee and Regierungspraesident of Koeln, and is in compliance with the German laws for animal protection. Five female cats in the weight range 2.8–5.0 kg (mean 3.4 kg) were studied. Premedication was with ketamine hydrochloride (25 mg/kg intramuscularly) and after cannulating the left femoral artery and vein, the animals were tracheotomized and immobilized with pancuronium bromide (0.2 mg/kg i.v.). For preparatory surgery, artificial ventilation was initiated and anaesthesia was changed to halothane (1–2% in a 70% nitrous oxide/30% oxygen gas mixture). Maintenance anaesthesia was with α-chloralose (Sigma-Aldrich, Germany) given as an initial intravenous infusion (60 mg/kg) at 60°C over 5 min, with cessation of halothane, followed by maintenance at 5 mg/kg/h started 3 h after the initial bolus. Maintenance intravenous fluid was Ringer's solution (147.1 mM NaCl/4.0 mM KCl/2.25 mM Ca(2+)) at 3 ml/h containing gallamine triethiodide (5 mg/kg/h). Acid–base balance was controlled as described for Laboratory 1. Pool temperature was maintained with a servo-controlled electrical heating element, and transorbital MCAO was accomplished with an implanted device for remote occlusion (Graf *et al.*, 1986; Ohta *et al.*, 1997).

Recording of cortical DC-potential

Laboratory 1: To minimize artefactual induction of PIDs from presence of intracortical electrodes, two, or one, ball electrodes of chlorided silver ~2 mm in diameter were suspended via a coiled spring lead and placed on the posterior SG and/or MG (data not shown).

Laboratory 2: One, two or three twin-barrel microelectrodes were inserted into the SG and MG (ion-selective data will be reported separately). Potential in their reference barrel was measured against a sintered silver/silver chloride electrode in the subcutaneous tissue of the neck.

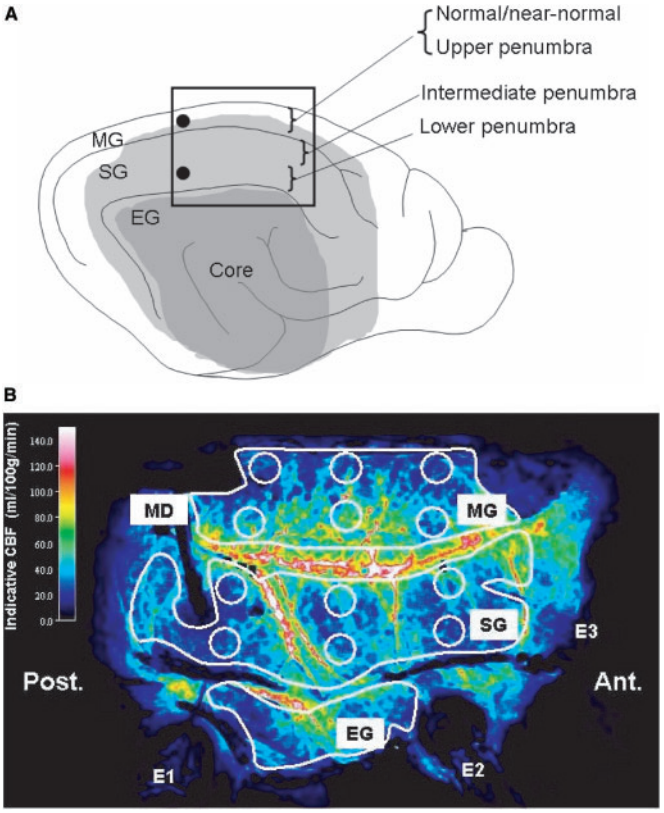

Fig. 1 (**A**) Diagram of the lateral aspect of the right hemisphere of the cat brain to illustrate typical gyral anatomy of ischaemic core (heavy shading) and penumbra (light shading) within the area exposed for imaging (rectangle), showing locations of nominal levels of penumbra and typical locations of DC surface or micro-electrodes (filled circle). (**B**) Typical pseudocolour transform of grey level perfusion image (Laboratory 2 experiments), calibrated here only for indicative perfusion (ml/100 g/min) (Strong *et al.*, 2006), illustrating (i) gyral anatomy of exposed hemisphere (MG/SG/EG), (ii) whole gyrus ROIs outlined (white) so as to exclude microelecrodes (EI–3), one microdialysis (MD) probe used additionally in this particular experiment and (iii) typical lateral and medial, anterior, intermediate and posterior locations and sizes of ROIs for extraction of perfusion time courses during transient perfusion events. These latter are illustrated here with graphics software as circles, but for actual data analysis were drawn freehand and ~60% of area illustrated, so as to avoid vessels and optimize time resolution.

Image acquisition and post-processing (both laboratories)

The laser speckle imaging method was implemented in this experimental system as recently described (Strong *et al.*, 2006). Briefly, the cortex was illuminated with a laser diode (Sanyo DL7140-201, 785 nm, 70 mW) via a diverging lens at a distance of 12–20 cm from the cortex. Scattered light was imaged at the narrowest available aperture setting (nominal f22) with a Peltier-cooled CCD camera (CT150A, CTec Photonics, Modesto, CA, USA), and images digitized to 8 bits with a LG-3 card

(Scion Corporation, Frederick, MD, USA), giving a (cortical) pixel size of ~29 × 29 μm. Software was written in-house ('C') to allow derivation of an image of the inverse of the calculated laser speckle contrast (inverse correlation time, ICT), and implemented on a 2.6 GHz Xeon processor. Since laser speckle contrast is inversely proportional to perfusion, inversion of the speckle image yielded an image whose grey level we have shown is a linear function of perfusion at least from ischaemic up to normal levels (Strong *et al.*, 2006). Processor time required for the calculation resulted in a time interval between images of some 13 s, and in later experiments 7.5 s. For analysis of the impact of PID-linked reductions in perfusion on the cortex, an appropriate number of small (typically 0.25–0.4 mm^2) regions-of-interest (ROIs) were drawn. For sample estimates of propagation rate, image magnification was calibrated with a 5 mm target placed in the image field. To assess overall trends in perfusion in whole gyri, three large ROIs were drawn, each mapping the entire exposed section of the EG, SG, MG. Since in the cat brain these gyri radiate concentrically at progressively increasing distances from the middle cerebral artery, they are for ease of reference designated alternately [and on the basis of earlier work (Strong *et al.*, 1983)] here as core (EG), low penumbra (lateral SG), intermediate penumbra (medial SG), upper penumbra (lateral MG), normal/near-normal (medial MG) (Fig. 1A).

In order to assess the true magnitude and hence the potential impact of PID-linked reductions in perfusion on cortical viability, we derived an '*indicative*' value of perfusion in absolute units from the equation: CBF (ml/100 g/min) = (ICT-650)/273. This manoeuvre and expression are based on the use throughout these experiments of speckle imaging optics and acquisition routines identical with those used for our earlier report specifically comparing ICT with perfusion as imaged quantitatively with the umbelliferone clearance method (Strong *et al.*, 2006). (Specific calibration of speckle against umbelliferone clearance was undertaken only in the first three experiments in Laboratory 1: calibration data were reported in detail as experiments 2–4 in the paper cited earlier.) This allowed comparison of image grey levels with long-established perfusion thresholds for sustained depolarization likely to indicate infarction (Strong *et al.*, 1983). Thus we here report perfusion values primarily in raw values of ICT, but also in units of ml/100 g/min, to allow some assessment of the true magnitude and pathological implications of the changes observed.

Termination of experiments

Experiments were terminated by perfusion–fixation (Laboratory 1: neuropathological findings will be reported separately) or by intravenous KCl injection (Laboratory 2: detection of terminal depolarization after KCl injection served as confirmation of proper microelectrode function)

Analysis of perfusion data

Two types of analysis were undertaken. First, one large ROI was drawn freehand for each of the three gyri exposed, but excluding pixels occupied by electrodes and their connections. Time series mean perfusion data for each gyrus were extracted to provide information on overall trends in perfusion. Secondly, in order to examine the time course of perfusion associated with individual depolarization events at specific small foci, small ROIs were drawn freehand (so as to avoid surface blood vessels), three each on the three penumbral and on the normal/near cortical 'ribbons' designated earlier. ROIs were sited anterior and posterior on each ribbon, and approximately mid-way between these (typical locations and approximate size are illustrated by small circles in Fig. 1B). This approach was prompted by the observation of apparent differences in perfusion dynamics between medial (anterior and likely posterior cerebral artery territory) and lateral (middle cerebral artery) locations on the MG, and occasional similar differences on the SG.

Statistical methods

CBF data for whole gyri was examined with analysis of covariance, using time points −5 and 0 min as covariates. The data were analysed on the log scale, so as to satisfy the two assumptions of ANOVA—that groups have similar variance and that the variability of the response is similar across the range of the response. Fisher's Least Significant Difference test was used to test for differences in time points:

(i) ten minutes after MCAO versus later time points for the core (EG) and lower/intermediate (SG) penumbral gyri,
(ii) core (EG) versus lower/intermediate penumbral (SG) at each time point,
(iii) lower/intermediate penumbral (SG) versus upper penumbral/normal/near-normal (MG) at each time point.

CBF data for small focal ROIs were highly variable both spatially and temporally, and both within and between experiments. An approach was required which served to rationalize but not to obscure variability. Therefore, each transient perfusion event in each focal ROI was treated as an independent observation, acknowledging that a single event that propagated throughout the entire penumbra SG and MG would necessarily be assessed at 12 different locations. Perfusion events were classified into four categories on the basis of their time course at the different locations that they invaded, as described in the 'Results' section.

Results

Unless otherwise stated, results are from Laboratory 1.

Systemic variables

Arterial blood gases remained substantially stable (Table 1), but there was a tendency for MAP to decline gradually in Laboratory 1: initial mild hypertension was controlled by withdrawal of blood in two experiments. Haematocrit fell during experiments from 39 ± 5 to 34 ± 6%; this is

Table 1 Arterial blood gases (Laboratory 1)

Hours after occlusion		−1	0	1	2	3	4
pH	Mean	7.36	7.35	7.35	7.33	7.34	7.35
	SD	0.03	0.03	0.03	0.04	0.05	0.04
pCO_2	Mean	29.6	31.4	30.9	31.5	32.1	31.5
	SD	1.9	2.4	1.8	2.8	3.1	4.3
pO_2	Mean	116	111	127	119	118	119
	SD	16	14	45	23	9	14

attributable to effects of intravenous infusion throughout all experiments. Arterial pressure tended to run lower in Laboratory 1 than in 2, with a difference of ~20 mmHg.

Baseline values of perfusion

A whole (exposed) hemisphere value of pre-ischaemic CBF was calculated for each experiment as the mean of three gyri. Overall group mean ICT was 11707 ± SD 4581, equivalent to 40.5 ± SD 14.4 ml/100 g/min.

Immediate effects of middle cerebral artery occlusion, and early collateralization

There was an immediate fall in perfusion (Fig. 2), visible in the first image after occlusion, to 5318 ± 2916 (equivalent to CBF ~17.1 ± 8.3 ml/100 g/min), 5291 ± 3407 (CBF ~17.0 ± 10.1) and 6711 ± 3271 (CBF ~22.2 ± 9.6), recovering after 10 min to 8704 ± 4581 (CBF ~29.5 ± 14.4), 9741 ± 4499 (CBF ~33.3 ± 14.1) and 10 314 ± 3762 (CBF ~35.4 ± 11.4) on the core (EG), lower and intermediate penumbral (SG) and upper penumbral/normal/near-normal (MG), respectively.

Patterns of delayed change in perfusion (20–240 min post-MCAO)

In the series taken as a whole, there was a striking trend for perfusion to fall secondarily, on the two gyri nearer the middle cerebral artery, significant ($P < 0.01$, Fisher's LSD) on the core gyrus from 60 min and in low and intermediate penumbra from 90 min onwards (compared with perfusion 10 min after MCAO), but the severity and also the time course of this change varied greatly in different experiments. Overall, perfusion 4 h after MCAO was maintained near pre-occlusion levels on the marginal gyrus (upper penumbra/normal/near-normal), at 11 625 ± 5892 ICT units, equivalent to CBF ~40.2 ± 19.2, but had fallen on middle/lower penumbra to 7830 ± 4336 (CBF ~26.3 ± 13.5), and in the core to 5509 ± 4363 (CBF ~17.8 ± 13.6 ml/100 g/min). From 60 min onwards, perfusion in the core was significantly lower than in middle/lower penumbra ($P < 0.01$), and in turn lower here than in upper penumbra/normal/near-normal from 120 min.

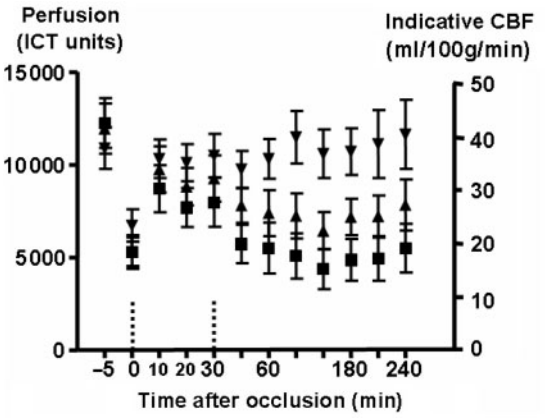

Fig. 2 Time course of perfusion (ICT units) [equivalent indicative CBF scale (ml/100 g/min) is shown on the right] on three gyri (filled square: EG, or core; filled triangle: SG, or lower and intermediate penumbra; filled inverse triangle: MG, or upper penumbra and near-normal or normal cortex) before, at and after MCAO. There is rapid development of collateral perfusion on all gyri within 10 min, but secondary falls in perfusion in the SG (filled triangle: $P < 0.01$ from 90 min onwards) and EG (filled square: $P < 0.01$ from 60 min) (compared with perfusion 10 min after occlusion). Dotted vertical bars indicate changes in scaling of the time axis.

Transient changes in perfusion (please refer to website video material)

Assessment of the time course of transient, propagating changes in perfusion was undertaken on the basis of detailed and repeated viewing of the image sequences as time lapse videos. Two examples of such video material are available on the *Brain* website as files Strong_et_al1.mp4 and Strong_et_al2.mp4, and they are described here. Both are time lapse sequences of laser speckle perfusion images, pseudocolour transforms of the ICT grey-level images. The views are predominantly of the penumbral cortex, exposed under oil: the peripheral areas of low perfusion (blue) lie beyond the area of brain exposure, and the anatomical labelling is given in Fig. 1A: what is exposed of the core gyrus is lowermost, with the normal/near-normal gyrus uppermost in the images. A scale bar (5 mm) and the ROIs label the first image in the sequences. '*Video 1*' (Strong_et_al1) was recorded 180 min after MCAO and lasts 13 min 48 s. A hypoperfusion event commences at a focus near the edge of an area of low perfusion, and spreads onto, medially and forwards on the area of lower and intermediate penumbra (SG). Propagation speed from ROI A to B was 3.05 mm/min; in this area the fall in perfusion (expressed as indicative perfusion) is below classical tissue viability thresholds, and is not reversed, thus representing an expansion of core territory. The perfusion event meanwhile descends into a sulcus for 186 s before emerging onto the outer penumbral/near-normal (marginal) gyrus, again as hypoperfusion but now of much shorter duration than on the lower penumbra, and fully reversible. Note: the primary propagating perfusion event is hypoperfusion, which is not preceded by any hyperaemia that could cause any steal from the region subject to hypoperfusion. The start of the sequence is marked by the longer-displayed frame with the millimetre calibration bar and ROIs. '*Video 2*' (Strong_et_al2) was recorded between 3 and 12 min after MCAO. A hypoperfusion event commences on the lower/intermediate penumbra (SG) and propagates backwards, first on this gyrus, then on the core gyrus and on the upper penumbral gyrus, apparently after a delay required to invade these two gyri across the intervening sulci. Propagation speed between ROIs was 3.10 mm/min. Note: (i) loss of definition of surface vasculature during hypoperfusion, suggestive of (but not clearly

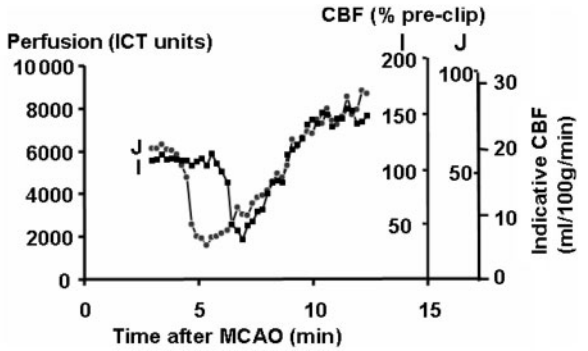

Fig. 3 Time course of perfusion in ROIs I–J in Video 2 (Strong.et.al2.gif) (lower penumbra: lateral SG), showing propagation of a peri-infarct depolarization within 3 min of MCAO. Derived axes are shown to the right (CBF reactivity is referenced to 5 min mean pre-occlusion: these baselines differed in the two ROIs but converged after occlusion). As it propagates from ROI-J to I (velocity 3.10 mm/min), the PID is associated with a marked primary fall in perfusion, followed by hyperaemia; this indicates that sufficient collateral perfusion is available to support hyperaemia in these ROIs, making steal an unlikely explanation for the primary hypoperfusion response.

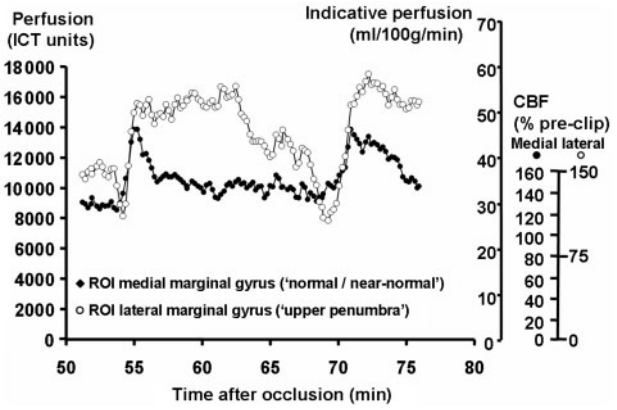

Fig. 4 Comparison of time courses of perfusion change (two-point running mean) in adjacent medial (filled circle) (anterior cerebral artery territory: normal or near-normal tissue) and lateral (open circle) (middle cerebral artery territory: upper penumbra) ROIs on the anterior marginal gyrus, during posterior to anterior propagation of two peri-infarct depolarizations (% CBF reactivity was scaled separately for the two ROIs, referenced to the mean pre-occlusion values). Although in the first event there is a marked increase in perfusion in the medial ROI that might be thought responsible for steal from the lateral ROI, in the second event the reduction in lateral perfusion occurs when perfusion in the medial ROI has yet to increase, suggesting primary vasoconstriction in the lateral ROI rather than steal (the subsequent lateral hyperaemia indicates the presence of sufficient collateral potential to support hyperaemia here, excluding steal in the hypoperfusion phase).

demonstrating) vasoconstriction, (ii) as in Video 1, the primary propagating perfusion event is hypoperfusion, which is not preceded by any hyperaemia (illustrated in Fig. 3).

The considerable variability in the geographical extent of propagation of transient changes in speckle signal, the

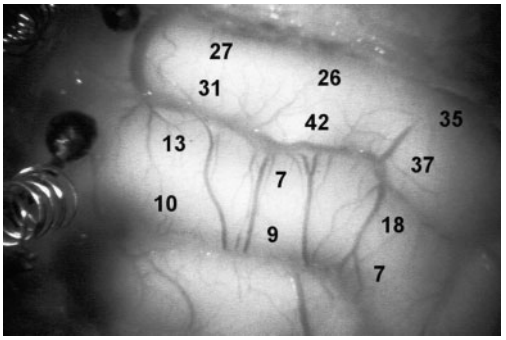

Fig. 5 Locations for analysis of transient changes in perfusion (plain image of exposed right hemisphere cortex). The numbers at each gyral location indicate the absolute, aggregate number of transient perfusion changes (Types A–D taken together) detected with speckle imaging that occurred in all Laboratory I experiments ($n = 14$) at that location. A total of 74 events occurred. Frequencies of different patterns of transient events (Types A–D) at the different locations are shown in Table 2.

differences in quality of collateral perfusion (especially in upper penumbral/normal/near-normal), and the additional heterogeneity in time all presented considerable challenges in analysis of the data. For example, a single event propagating over upper penumbra/normal/near-normal soon after MCAO might be associated with transient hyperperfusion, but a later event affecting the same ROIs, with hypoperfusion laterally and hyperperfusion medially (Fig. 4). Since extra information would emerge, we therefore elected to designate small medial and lateral ROIs in this heterogenous territory (maximum 6). On the lower/middle penumbral gyrus (SG), fewer were sometimes designated, as there was less medial–lateral heterogeneity, and, because of the progressive development of core conditions on this gyrus (Fig. 2), there were fewer transient events than in upper penumbra.

In the 14 experiments in Laboratory 1, a total of 74 transient changes in the speckle signal were observed. Most propagated throughout at least one gyrus, and sometimes throughout penumbra and normal/near-normal cortex, and were first classified according to four patterns of perfusion time course observed at the different small ROIs. The spatial distribution and occurrence of these different patterns is described later and is documented semi-graphically in Fig. 5—this figure documents at each gyral location the absolute number of perfusion transients (A, B, C or D) reaching each location (the total number observed in the Laboratory 1 experiments was 74, ranging in individual experiments between 0 and 11). In Table 2 we report the relative ease of propagation of Types A, B, C and D to the different gyral locations, expressed as a percentage of 74.

Monophasic increases in perfusion (Type A, Fig. 6)

Rapid, transient and monophasic 'increases' in perfusion associated with a propagating event occurred principally on

Table 2 Relative numbers of propagating perfusion events of different time courses in ROIs imaged in representative sites in penumbra (please see also Figs 5 and 6)

Location of ROI	Type of change	Posterior		Intermediate		Anterior	
		Absolute number of events at ROI	% of Type (A–D) at ROI	Absolute number of events at ROI	% of Type (A–D) at ROI	Absolute number of events at ROI	% of Type (A–D) at ROI
Normal/ near-normal (medial MG)	A	19	70.4	17	65.4	24	68.6
	B	8	29.6	8	30.8	10	28.6
	C	0	0.0	1	3.8	1	2.9
	D	0	0.0	0	0.0	0	0.0
	All†	**27**		**26**		**35**	
Upper penumbra (lateral MG)	A	12	38.7	14	33.3	11	29.7
	B	10	32.3	18	42.9	17	45.9
	C	9	29.0	10	23.8	9	24.3
	D	0	0.0	0	0.0	0	0.0
	All†	**31**		**42**		**37**	
Intermediate penumbra (medial SG)	A	0	0.0	1	14.3	0	0.0
	B	6	46.2	2	28.6	6	33.3
	C	7	53.8	4	57.1	11	61.1
	D	0	0.0	0	0.0	1	5.6
	All†	**13**		**7**		**18**	
Lower penumbra (lateral SG)	A	0	0.0	0	0.0	0	0.0
	B	5	50.0	2	22.2	2	28.6
	C	4	40.0	6	66.7	4	57.1
	D	1	10.0	1	11.1	1	14.3
	All†	**10**		**9**		**7**	

(i) Columns and rows are arranged so as to replicate for convenience the anatomical relativities in the exposed, ischaemic right cerebral hemisphere. (ii) Definitions: A (Fig. 6, Type A): rapid, monophasic 'increase' in perfusion (relative to pre-event perfusion) developing over 25–40 s (two or three image intervals). B (Fig. 6, Type B): biphasic, consisting of a transient fall in perfusion, again over 25–40 s, but followed by hyperaemia, typically lasting 5–10 min. C (Fig. 6, Type C): monophasic fall in perfusion (no reactive hyperaemia), lasting for some 5–60 min or longer. D (Fig. 6, Type D): large and essentially permanent fall in perfusion. (iii) Total number of events observed in the series is stated at each location: the overall total number of PIDs was 74: the figure in each % cell therefore indicates the relative susceptibility of that locus to involvement in the specific perfusion pattern (A, B, C or D). All†: (bold) total number of events at specified location (all types). (iv) Frequency of invasion of SG by perfusion events is lower than on MG, attributed to earlier onset of sustained depolarization in SG (recruitment into core), or of refractoriness to recurrent depolarization. (v) Although no permanent, propagating falls in perfusion (type D) were recorded in the lateral marginal gyrus, cumulative effects of incomplete recovery of perfusion led to focal, mild ischaemia at 4 h in several experiments.

the normal/near-normal ribbon of cortex (medial MG), developing over 25–40 s. Mean pretransient baseline perfusion in this group ($n = 94$) was 9796 ± 4472 (CBF $\sim 33.5 \pm$ SD 14.0 ml/100 g/min), rising to a peak of $14\,928 \pm 6711$ (CBF $\sim 52.3 \pm 22.2$ ml/100 g/min). There was a highly significant linear relationship between peak (ordinate) and baseline (abscissa) values of perfusion ($P < 0.0001$: x-intercept $= -2.9$: slope $= 1.40$). Hyperaemia occasionally occurred even when indicative baseline perfusion lay between 3926 ± 6110 (CBF ~ 12 and 20 ml/100 g/min).

Biphasic perfusion transients (Type B, Fig. 6)

This pattern—transient decrease in perfusion followed by an increase—was most characteristic of depolarization events affecting the lateral strip of the marginal gyrus. Perfusion first fell, over 25–40 s, then rose above baseline, this hyperaemia lasting typically 5–10 min. Mean pretransient baseline perfusion in this group ($n = 105$) was $11\,133 \pm 4417$ (CBF $\sim 38.4 \pm$ SD 13.8 ml/100 g/min), falling to 7202 ± 3435 (CBF $\sim 24.0 \pm 10.2$ ml/100 g/min), and rising to $15\,419 \pm 8813$ (CBF $\sim 54.1 \pm 29.9$) in the hyperaemic phase. Recovery of perfusion to baseline was typically complete within 2–3 min. As with Type A events, there was an apparent linear dependence of hypoperfusion (slope 0.61, $P < 0.0001$) and later of hyperperfusion (slope 1.2, $P < 0.0001$) on initial baseline perfusion. In a significant proportion (38%, Table 2) of Type B events occurring in the normal/near-normal ribbon, perfusion fell briefly to values which, when they remain low, have been associated in the past with large, sustained increases in extracellular K^+ concentration in this stroke model (Strong *et al.*, 1983). The subsequent development of hyperaemia indicates that a fall in perfusion to below a certain level is not by itself a critical factor in determining the subsequent time-course of perfusion.

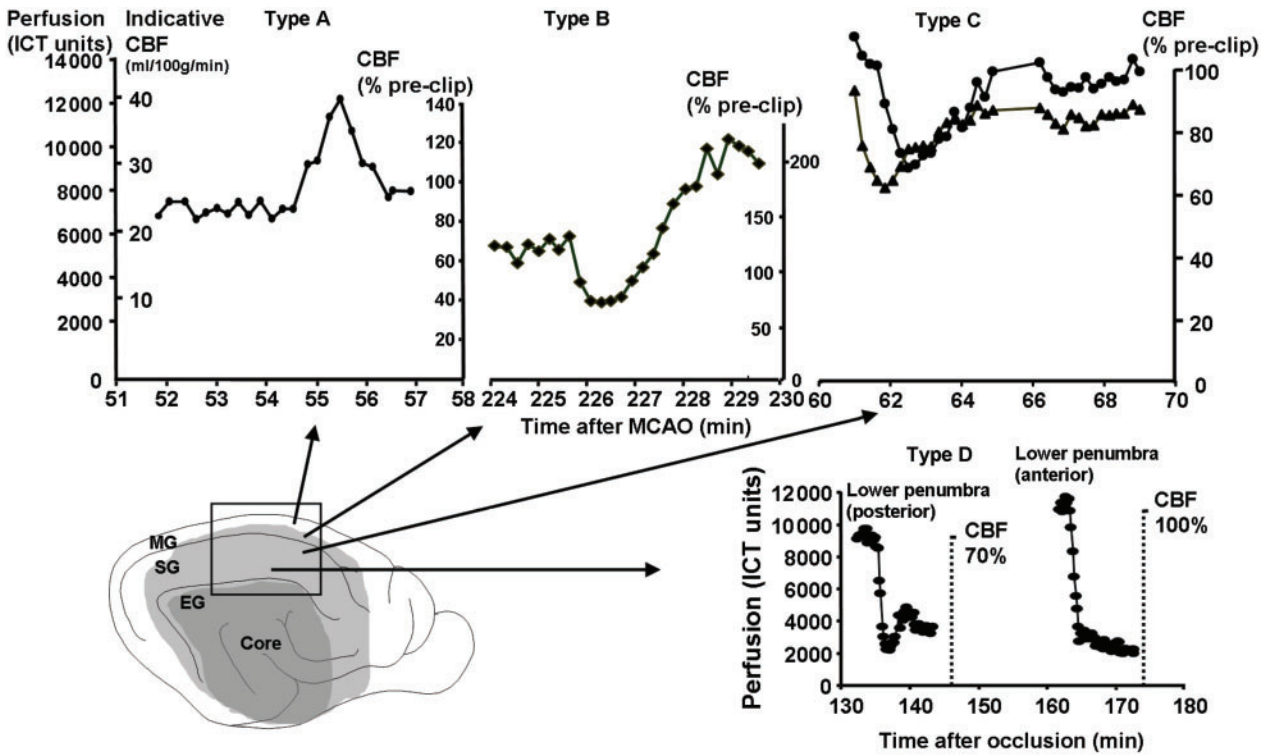

Fig. 6 Examples of four different patterns of transient (A, B, C) and permanent (D) change in perfusion that propagate in penumbral or near-normal gyri. For upper three panels, ICT and indicative CBF scales are shown to the left, and individual reactivity scales to the right of each figure. Type A: monophasic transient increase in perfusion, typical of near-normal/normal cortex (unshaded, medial ribbon of MG uppermost in diagram, perfused largely by the anterior cerebral artery). Type B: biphasic, consisting of a transient fall in perfusion (approximate half-time for recovery to baseline 0.5–1.5 min), followed by hyperaemia, typically lasting 5–10 min, typical of upper penumbra (shaded portion of MG in diagram). Type C: monophasic transient decrease in perfusion, with varying rate of recovery, which was sometimes incomplete, approximate half-time 2–30 min. The panel illustrates effects on perfusion of a single Type C event propagating forward through two ROIs, here in upper penumbra (lateral MG): calculated propagation velocity was 2 mm/min. Type C events were more typical of intermediate penumbra, as illustrated by arrow. Type D: examples of abrupt, marked falls in perfusion, with no or minimal recovery, associated here with two separate spreading events, some 40 min apart, on lower penumbra; indicative CBF fell to ~10 ml/100 g/min, i.e. core conditions. Dotted calibration bars indicate CBF change as percentage pre-occlusion.

Monophasic decreases in perfusion (Type C, Fig. 6)

Transient falls in perfusion associated with a propagating event, again of rapid onset, but not followed by relative hyperaemia were commonest on the intermediate and upper penumbral ribbons of cortex. Mean pretransient baseline perfusion in this group ($n = 43$) was $12\,580 \pm 6711$ (CBF ~$43.7 \pm$ SD 22.2 ml/100 g/min), falling to 6629 ± 4254 (CBF ~21.9 ± 13.2 ml/100 g/min). There was a highly significant linear relationship between minimum (ordinate) and baseline (abscissa) values of perfusion ($P < 0.0001$: x-intercept $= -3.6$: slope $= 0.46$). Perfusion fell below putatively 'critical' values in more than 50% of Type C events in lower and intermediate penumbra. Recovery required between 3 and 60 min, and was not always complete, or was overtaken by a second Type C event.

Sustained falls in perfusion (Type D, Fig. 6)

This pattern of irreversible fall in perfusion in association with a propagating event was characteristic of intermediate and lower penumbra, and was necessarily limited in number, never being repeated at the same locus. Perfusion fell in these events from 9140 ± 5045 (CBF ~$31.1 \pm$ SD 16.1) to 3162 ± 2261 (CBF ~9.2 ± 5.9 ml/100 g/min). As with events of Types A, B and C, there was a significant, linear dependence of post-event perfusion on the baseline value (slope 0.29, $P = 0.001$). Thus, fall in perfusion became progressively greater in Types C and D events compared with Type B, for any given level of baseline perfusion.

Transient changes in perfusion in relation to cortical parenchymal DC potential (microelectrode) (Laboratory 2)

In order to examine the possibility that a propagating fall in perfusion might be the primary event, causing depolarization as a 'result' of ischaemia, we assessed relative timing of the two events, by comparing time of first fall in DC potential with first change in perfusion in small ROIs drawn over the electrode tip. We made measurements in

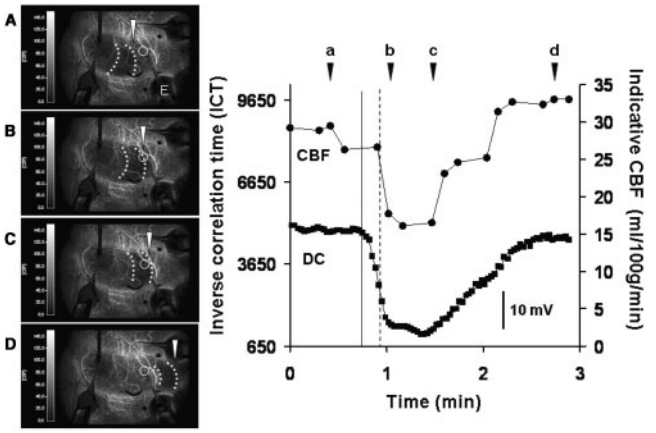

Fig. 7 Relative timing of DC potential (depth microelectrode, Laboratory 2) and perfusion transient events. Consecutive images (**A**–**D**, taken from a video clip) show the propagation of transient hypoperfusion, bounded by dotted lines, in relation to the circular ROI, which was drawn at the tip of a microelectrode. The graph on the right shows the DC recording obtained with the microelectrode and corresponding CBF values obtained by evaluating the circular ROI at the tip of the electrode. Arrowheads show time points corresponding to images **A**–**D**. Solid vertical line shows onset of DC shift, dashed vertical line shows the last point before CBF reduction thus documenting a delay of the perfusion wave of around 10–15 s.

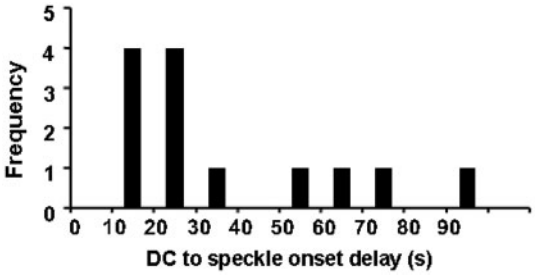

Fig. 8 Histogram of the frequency distribution of the delay (seconds) between first onset of depolarization at a cortical microelectrode and onset of change in cortical perfusion in peri-infarct depolarizations. Recording system clocks were synchronized to within 2 s: perfusion sampling interval was 8 s. The delays in all cases between depolarization and change in perfusion indicate that under these conditions change in perfusion is an effect rather than a cause of depolarization.

five separate experiments, recording the DC potential from one channel of a double-barrel microelectrode. The modal delay from depolarization to onset of change in perfusion was 10–30 s (Figs 7 and 8), confirming that depolarization leads to loss of perfusion rather than the reverse.

Discussion

To our knowledge this is the first full report of inverse coupling of perfusion with propagating depolarization in the gyrencephalic brain. 'Inverse coupling' refers to a reduction of perfusion linked to depolarization, unlike the expected hyperaemia characteristic of Leão's CSD. We argue later that our results are best interpreted as indicating vasoconstriction in the cortical microcirculation. The sustained and severe nature of many of the propagating reductions in perfusion that we observed suggests that vasoconstriction linked to the depolarization is the basis of the dependence of infarct size on number of PIDs. This emphasizes again that PIDs are a fundamental component of the process of infarction rather than being an epiphenomenon. This finding is given added significance by the recent demonstrations of propagating episodes of suppression of amplitude of the ECoG in the cerebral cortex of patients who have suffered traumatic cerebral contusions (Strong *et al.*, 2002) or aneurysmal SAH (Dreier *et al.*, 2006); these events have now been shown to represent cortical depolarization (Fabricius *et al.*, 2006). Indeed, these clinical findings indicate two patterns of ECoG suppression event—either with normal resumption of ECoG activity after a few minutes (possibly benign), or with much delayed or absent recovery of ECoG amplitude (Fabricius *et al.*, 2006). This latter pattern is believed to represent the clinical analogue of PIDs. Most particularly, Dreier *et al.* now report evidence in patients with SAH of clinical and radiological deterioration linked closely with clusters of depolarization events, some of which show evidence of deterioration with time from full to absent ECoG amplitude recovery (Dreier *et al.*, 2006). After review here of the scientific context and the methods on which the present findings are based, the patterns of perfusion change and their interpretation in terms of the underlying vascular events, the discussion will conclude with brief consideration of the novel implications for understanding of delayed deterioration in patients with acute cerebral ischaemia, especially that following aneurysmal SAH.

Introduction of the laser speckle method for imaging of cerebral cortical perfusion (Dunn *et al.*, 2001) has for the first time provided a means of monitoring cortical perfusion with sufficient temporal and spatial resolution to allow more detailed exploration of the relationship between propagating depolarization events and perfusion: in particular it allows frequent sampling of perfusion throughout the exposed area of cortex. Initial experience with the method in cats undergoing MCAO suggested that PIDs might be associated with striking 'reductions' in perfusion (Strong *et al.*, 2003), and application of this method in studies of MCAO in mice indicates that enlargement of the infarct proceeds in a series of steps, each linked to a PID (Shin *et al.*, 2006). Demonstration of a linear relationship of the laser speckle ICT with values of perfusion based on indicator clearance (within the range from ischaemic up to normal flows) now allows us to assign greater pathophysiological significance to the reductions in perfusion that we saw than would be possible from raw ICT data alone (Strong *et al.*, 2006). The present, detailed study demonstrates clearly that

under penumbral conditions, PIDs (as defined at the start of these experiments by a change in perfusion propagating at a speed compatible with that of spreading depression) are indeed often characterized by—and, as argued later, most probably 'cause'—rapid reductions in perfusion of varying severity and duration that increasingly threaten tissue viability as they recur.

Review of methods

Introduction of laser speckle imaging of perfusion has yielded a large volume of extra information on the patterns of spread of transient and sustained events in the ischaemic penumbra that would not be available from measurements from probes or electrodes necessarily placed at fixed locations. However, the image acquisition rate available in this study (13 and later 7.5 s) may have failed to resolve brief perfusion changes (of either polarity). In addition, the laser speckle method samples mean red cell velocity, and is not a 'direct' measure of perfusion in the microcirculation; however, in practice the method samples both velocity and volume, and our earlier calibration study indicates a linear relationship between inverse laser speckle correlation time and perfusion in the range between marked ischaemia and normal perfusion, although it did not examine hyperaemia (Strong *et al.*, 2006). Both the ICT and the indicative absolute CBF values reported here for hyperaemia must therefore be interpreted with caution. Nevertheless, the varying patterns of perfusion change observed here will be available as sample 'signatures' for reference during clinical monitoring of perfusion in patients with acute cerebral ischaemia. The alternative expression of perfusion values as 'indicative CBF' serves, importantly, to emphasize that in some instances the reductions in perfusion associated with depolarizations are very substantial, and, when irreversible, most probably lethal to the area of cortex affected.

Transient changes in perfusion

Hyperaemic (dilator) responses

Hyperaemia or other indices suggesting vasodilation are very well recognized as the initial response of the healthy cerebral circulation to CSD. Our 'Type A' response appears to be an example of this (probably attenuated in comparison with normally perfused cortex), developing in the best-perfused ribbon of cortex within the exposed territory—the medial marginal gyrus (normal/near-normal)—when the propagating wave reaches it. Detailed review of candidate dilator mechanisms such as adenosine, nitric oxide or eicosanoid derivatives is not appropriate here, and we make no assumption as to whether the mechanism of intense vasodilation to CSD in the normally perfused brain differs 'qualitatively' from that of functional activation, or simply represents modulation of a single mechanism. The increase to 140% (regression of peak on baseline: slope = 1.4) or 156% (mean peak as % mean baseline) in Type A events after MCAO is considerably less than we have seen in unpublished studies of endothelin-induced CSD (without vascular occlusion), where hyperaemia ranged from 162% to 433%. An earlier study of CSD in the same species reported mean hyperaemia of 215% (Piper *et al.*, 1991). Whether our values for perfusion response in normal/near-normal cortex after MCAO represent limitation by diminished collateral or a change in a component of the coupling mechanism is not clear.

Patterns of transient and sustained reductions in perfusion coupled to depolarizations after middle cerebral artery occlusion

Our data suggest three patterns of transient reduction in perfusion that propagate in the middle cerebral territory [(i) transient increase, as discussed earlier, (ii) biphasic, i.e. decrease followed by an increase, (iii) monophasic decrease]. The description of the three patterns of transient change is, to a large extent, a matter of convenience, and could arguably be interpreted as simultaneous but independent hypoperfusion and dilator responses, present to varying degrees and progressing with different time courses. However, we do not believe that the time series data are of sufficient quality or time resolution to merit formal decomposition into two components.

In a fourth pattern, a substantial and permanent fall in perfusion propagates widely (Video 1: Strong_et_al1); the effect of such an event is—within a matter of minutes and sometimes after a considerable delay after MCAO—to reduce perfusion in an entire gyrus to below levels thought necessary to preserve viability or the potential for later recovery of function. The time course of perfusion in this fourth response closely resembles that of DC potential or extracellular K^+ in anoxic or terminal depolarization, and invites speculation on the precise chain of events in terminal depolarization. Reduction in perfusion linked to depolarization adds a further challenge to tissue viability, additional to decline in tissue glucose linked to PIDs, and to an increase in frequency of spontaneous PIDs, itself reflecting, in part, increased glycolysis, reduced glucose availability, and, by implication, compromised regulation of extracellular cation and neurotransmitter levels (Hopwood *et al.*, 2005).

The mechanism of reductions in perfusion linked to PIDs

We address first the relative timing of the electrophysiological and vascular events, and then the mechanism of the falls in perfusion that were observed.

Is depolarization or perfusion loss the primary event in PIDs?

Since reduction of perfusion, whether by proximal occlusion or systemic hypotension, is well-known to cause depolarization by reduction of CBF below critical thresholds (Astrup *et al.*, 1977), it is important to establish the chain of causality underlying the observation of a reduction in perfusion that propagates across the cortex with a velocity characteristic of spreading depression—a cardinal feature of a PID. Are we observing an effect of depolarization on perfusion, or a propagating reduction in perfusion that causes ischaemic depolarization? To address this question, we examined the relative timing of the two events, in two experimental systems, recording DC potential either with 2 mm spherical electrodes on the cortical surface (Laboratory 1) or with intracortical microelectrodes (Laboratory 2). Surface electrode data from Laboratory 1 (not shown) suggested that depolarization leads to a reduction in perfusion rather than the reverse, and this was shown formally in Laboratory 2 with microelectrodes, with a modal delay of 10–30 s (Figs 7 and 8). Shin *et al.* reported a delay of <10 s (always depolarization first) in five mice (microelectrode study) (Shin *et al.*, 2006) Thus depolarization leads to rather than follows the vascular response, propagating across the cortex ahead of it. This temporal relationship is an essential element in the emerging concept of vasoconstrictive depolarization in pathological conditions (Dreier *et al.*, 2000; Shin *et al.*, 2006), which is elaborated later.

The argument for vasoconstriction in the microcirculation as the mechanism of perfusion loss linked to PIDs

In principle, three candidate mechanisms might account for reductions in perfusion linked to depolarizations: (a) steal linked to paralysis of autoregulation, (b) an abnormal response of the neurovascular coupling mechanism to depolarization—vasoconstriction or (c) microvascular compression from swelling of astrocytic foot processes.

(a and b) Steal and/or paralysis of autoregulation, or active vasoconstriction? When these experiments commenced, we expected that the method would provide confirmation that little or no increase in perfusion occurs at a given cortical locus in the penumbra upon arrival of a depolarization event, on the basis that the microcirculation is likely already to be maximally vasodilated—effectively resulting in paralysis of autoregulation. It would follow from this notion that the cytotoxicity of PIDs and their incremental effect on infarct size is due to the additional metabolic load imposed, uncompensated by hyperaemia. This in turn would, for example, prolong the adverse effects of increased free intracellular calcium ion (Siesjo, 1992). In relation to possible steal, the use of serial laser speckle imaging sequences viewed as time lapse videos allows assessment of the state of perfusion on either side of the depolarization as it propagates. Careful and repeated viewing of the video material available on the *Brain* website and linked to this paper (videos Strong_et_al1 and *2) is advised in considering the argument we now propose as follows.

A rapid reduction of perfusion in a zone of ischaemic, non-autoregulating cortex in the low or intermediate penumbra (SG) as reported here might occur under two circumstances. First, a reduction in systemic arterial perfusion pressure will reduce perfusion. However, such a change must necessarily occur '*simultaneously throughout*' the penumbra (although perhaps graded in severity, reflecting distance from collateral perfusion sources), rather than '*propagating*' at the same speed as CSD/PID, as is observed here. Second, and critically, a wave of hyperaemia propagating away from the middle cerebral artery input in association with CSD/PID might generate steal from cortex nearer the middle cerebral artery input. This would result in a reduction in perfusion that would '*follow*' the primary hyperaemia outwards from the MCA. The time course of perfusion in a cortical ROI affected by such a sequence during passage of a depolarization wave would be biphasic: hyperaemia then hypoperfusion. No such biphasic event was seen (Videos 1 and 2 illustrate the patterns we saw); rather, what propagates is a sustained [Strong_et_al1: (type D)] or transient [Strong_et_al2: (type B)] '*reduction*' in perfusion. In both videos, the time course of perfusion in two ROIs (A–B in Video 1 or J–I in Video 2) in the path of the spreading event as it affects the lower and intermediate penumbra is clearly seen. The hypoperfusion is the primary propagating event and is not preceded by any hyperaemia that could cause steal in a non-autoregulating vascular bed. The time course of perfusion in ROIs I and J in Video 2 is documented in Fig. 3. We argue that where no preceding hyperaemia is seen (as illustrated in both videos), this '*primary*' loss of perfusion propagating at the speed of CSD can only be explained by primary vasoconstriction in the microcirculation propagating as a consequence of the depolarization event.

Transient loss of definition of the surface vessels in the speckle images during the hypoperfusion transient as seen in Video 2 may be due to transient vasoconstriction, but, regardless of this, specific serial imaging of vessel calibre and perfusion in the microcirculation, preferably in conjunction with an index of depolarization, would be required to confirm the above argument.

(c) External compression of the microcirculation by swollen astrocyte foot processes was suggested as a mechanism of secondary deterioration and ischaemia (Bullock *et al.*, 1991; Schroder *et al.*, 1995), but whether the degree of swelling that is observed can account for the reduction in vascular calibre is open to question and requires study, and those who have studied the optical appearances of the cerebral microcirculation in response to depolarization *in vitro*

consider this an inadequate explanation (G. Carmignoto and B. McVicar, personal communications, 2005).

To summarize, we argue that vasoconstriction appears the most likely basis for perfusion loss accompanying PIDs. Specific confirmation of this reasoning by direct imaging would be desirable, but it is nevertheless in line with the conclusions of other authors, as follows.

Existing published evidence for vasoconstrictor responses linked to depolarizations

Evidence for perfusion loss coupled with propagating depolarization and attributed to vasoconstriction comes first from a group of papers from Dreier and colleagues, who superfused the cerebral cortex of rats with artificial CSF with a composition designed to simulate conditions likely to be present in patients following SAH. Monitoring perfusion and DC potential at two sites with laser Doppler probes and microelectrodes, respectively, they found evidence of reduction in perfusion associated with depolarization, and described the combination of findings as 'cortical spreading ischaemia' (Dreier *et al.*, 2000). Using microscopy, they confirmed vasoconstriction specifically (Dreier *et al.*, 1998). Next, Shin and her colleagues have assembled a persuasive body of evidence from the literature, cited together with their own findings in mice subject to acute MCAO, in support of the proposition that under pathological conditions a wave of cortical depolarization can lead to vasoconstriction rather than to dilation; they illustrate the effects of what they describe as anoxic depolarization (rather than of a PID) on surface vessel calibre (Shin *et al.*, 2006). In the same paper, this group reported reductions in perfusion coupled to PIDs, as registered by laser speckle imaging in mice undergoing MCAO. In support of the role of PIDs in the pathogenesis of infarction, they showed that the cortical territory subject to a specific level of ischaemia enlarged with each recurrent PID (Shin *et al.*, 2006). Dual-photon *in vivo* microscopy also provides evidence for vasoconstriction in the cortical microcirculation linked to spreading depression (Nimchinsky *et al.*, 2006).

The nature of vasoconstrictor responses

In the context of *in vivo* experimental work, potential mechanisms of vasoconstriction in response to depolarization have been considered in detail by Dreier and colleagues, and by Shin *et al.*, in their work cited earlier (Dreier *et al.*, 1998; Shin *et al.*, 2006). That dilation occurs with CSD in the normally perfused cortex, despite rises in extracellular $[K^+]$ to some 60 mM, while constriction is the response to the same K^+ increase in focal ischaemia, may result from NO depletion: several demonstrations exist of constrictor responses or increased hypoperfusion to elevated $[K^+]$ or CSD in the presence of nitric oxide synthase inhibition (Dreier *et al.*, 1995; Fabricius *et al.*, 1995; Ayata *et al.*, 2004). Studying vascular responses to neural activity in the retina *in vitro*, Metea and Newman also concluded that NO levels might determine whether the response to depolarization is dilation or constriction; differing changes in vasoactive eicosanoid concentrations, influenced by NO concentration, were thought to contribute (Metea and Newman, 2006). Endothelin-1 is released in brain injury (Barone *et al.*, 1994), is a powerful cerebral vasoconstrictor (Yanagisawa *et al.*, 1988), and, when applied locally, has also been shown to elicit spreading depression (Dreier *et al.*, 2002*a*). Thus it is likely that the different patterns of response to depolarization that we observed reflect varying combinations and timings of responses of the different elements in the neurovascular unit, and their differing sensitivities to pathological conditions.

Role of PIDS in infarction in the gyrencephalic brain

We have shown that in the majority of experiments in this study of the penumbral territory in focal ischaemia in the gyrencephalic brain, quality of collateral perfusion developing by 10 min after occlusion was good, and above levels associated in this model with sustained depolarization and probable infarction. We have also shown a high incidence of PIDs; each was associated, principally when close to core territory, with a variable degree of loss of perfusion that was slow to recover: this slow recovery of perfusion after a depolarization is in turn vulnerable to further perfusion loss from a later PID. It would thus appear that the initial effect of proximal occlusion in a partially collateralized cortical circulation in the gyrencephalic brain is not necessarily to cause immediate terminal depolarization, but rather to sensitize the microcirculation to the effects of depolarizations, possibly through NO depletion in the vasoregulatory mechanism. Thus deterioration rather than enhancement of perfusion is the response to depolarization in the ischaemic penumbra—and often proceeds in a series of steps (Shin *et al.*, 2006). We interpret this combination of findings, together with the recent literature, as suggesting strongly that a spontaneously occurring depolarization, propagating in cerebral grey matter where vasoreactivity is impaired, is a more active and pathogenic process than previously thought, and plays a fundamental but not an exclusive role in the early evolution of infarction in ischaemic gyrencephalic cortex. Nevertheless, the present experiments also serve to re-emphasize the contributions of other mechanisms in the early maturation of focal ischaemic lesions in the cerebral cortex. Thus in several cases, perfusion loss was more gradual, and spatially more homogeneous: in most cases this was related to a fall in arterial pressure.

Implications for clinical management of acute brain injury (ischaemia/trauma)

In the case of major occlusive stroke, these findings also raise once more the question whether 'clean' pharmacological agents can be identified which are capable of abrogating peri-infarct depolarizations or—perhaps preferably—their associated loss of perfusion. For patients with SAH, and compatible with a role for proximal vasospasm in DIND after SAH, the present results demonstrate how proximal vascular occlusion can alter the responses of the cortical microcirculation to depolarization events from vasodilatation (a 'benign' 'response) to *hypo*perfusion-threatening viability. Clinical documentation of transient changes in perfusion analogous to those reported here is required. In the case of contusional head injury, where depolarizations are known to occur (Mayevsky *et al.*, 1996; Strong *et al.*, 2002), the incidence and extent of ischaemia is the subject of continued debate; thus clinical studies similar to those for SAH are required.

Acknowledgements

We thank Shionogi-GlaxoSmithKline LLC and HeadFirst for their support for this study, and Dr Mesbah Alam for generously supplying the microelectrodes for work in Laboratory 2. We thank Dr Stefan Vollmar for invaluable help in preparing the video material. Funding to pay the Open Access publication charges for this article was provided by Shionogi & Co Ltd, Japan.

References

Astrup J, Symon L, Branston NM, Lassen NA. Cortical evoked potential and extracellular K+ and H+ at critical levels of brain ischaemia. Stroke 1977; 8: 51–7.

Ayata C, Shin HK, Salomone S, Ozdemir-Gursoy Y, Boas DA, Dunn AK, et al. Pronounced hypoperfusion during spreading depression in mouse cortex. J Cereb Blood Flow Metab 2004; 24: 1172–82.

Back T, Ginsberg MD, Dietrich WD, Watson BD. Induction of spreading depression in the ischemic hemisphere following experimental middle cerebral artery occlusion: effect on infarct morphology. J Cereb Blood Flow Metab 1996; 16: 202–13.

Barone FC, Globus MY, Price WJ, White RF, Storer BL, Feuerstein GZ, et al. Endothelin levels increase in rat focal and global ischemia. J Cereb Blood Flow Metab 1994; 14: 337–42.

Branston NM, Strong AJ, Symon L. Extracellular potassium activity, evoked potential and tissue blood flow: relationships during progressive ischaemia in baboon cerebral cortex. J Neurol Sci 1977; 32: 305–21.

Bullock R, Maxwell WL, Graham DI, Teasdale GM, Adams JH. Glial swelling following human cerebral contusion: an ultrastructural study. J Neurol Neurosurg Psychiatry 1991; 54: 427–34.

Busch E, Gyngell ML, Eis M, Hoehn Berlage M, Hossmann KA. Potassium-induced cortical spreading depressions during focal cerebral ischemia in rats: contribution to lesion growth assessed by diffusion-weighted NMR and biochemical imaging. J Cereb Blood Flow Metab 1996; 16: 1090–9.

Dijkhuizen RM, Beekwilder JP, van der Worp HB, Berkelbach van der Sprenkel JW, Tulleken CA, Nicolay K, et al. Correlation between tissue depolarizations and damage in focal ischemic rat brain. Brain Res 1999; 840: 194–205.

Dreier JP, Korner K, Gorner A, Lindauer U, Weih M, Villringer A, et al. Nitric oxide modulates the CBF response to increased extracellular potassium. J Cereb Blood Flow Metab 1995; 15: 914–9.

Dreier JP, Korner K, Ebert N, Gorner A, Rubin I, Back T, et al. Nitric oxide scavenging by hemoglobin or nitric oxide synthase inhibition by N-nitro-L-arginine induces cortical spreading ischemia when K+ is increased in the subarachnoid space. J Cereb Blood Flow Metab 1998; 18: 978–90.

Dreier JP, Ebert N, Priller J, Megow D, Lindauer U, Klee R, et al. Products of hemolysis in the subarachnoid space inducing spreading ischemia in the cortex and focal necrosis in rats: a model for delayed ischemic neurological deficits after subarachnoid hemorrhage? J Neurosurg 2000; 93: 658–66.

Dreier JP, Kleeberg J, Petzold G, Priller J, Windmuller O, Orzechowski HD, et al. Endothelin-1 potently induces Leao's cortical spreading depression in vivo in the rat: a model for an endothelial trigger of migrainous aura? Brain 2002a; 125: 102–12.

Dreier JP, Sakowitz OW, Harder A, Zimmer C, Dirnagl U, Valdueza JM, et al. Focal laminar cortical MR signal abnormalities after subarachnoid hemorrhage. Ann Neurol 2002b; 52: 825–9.

Dreier JP, Woitzik J, Fabricius M, Bhatia R, Major S, Drenckhahn C, et al. Delayed ischaemic neurological deficits after subarachnoid haemorrhage are associated with clusters of cortical spreading depression. Brain 2006; 129: 3224–3237.

Dunn AK, Bolay H, Moskowitz MA, Boas DA. Dynamic imaging of cerebral blood flow using laser speckle. J Cereb Blood Flow Metab 2001; 21: 195–201.

Fabricius M, Akgoren N, Lauritzen M. Arginine-nitric oxide pathway and cerebrovascular regulation in cortical spreading depression. Am J Physiol 1995; 269: H23–9.

Fabricius M, Fuhr S, Bhatia R, Boutelle M, Hashemi P, Strong AJ, et al. Cortical spreading depression and peri-infarct depolarization in acutely injured human cerebral cortex. Brain 2006; 129: 778–90.

Graf R, Kataoka K, Rosner G, Heiss WD. Cortical deafferentation in cat focal ischemia: disturbance and recovery of sensory functions in cortical areas with different degrees of cerebral blood flow reduction. J Cereb Blood Flow Metab 1986; 6: 566–73.

Hopwood SE, Parkin MC, Bezzina EL, Boutelle MG, Strong AJ. Transient changes in cortical glucose and lactate levels associated with peri-infarct depolarisations, studied with rapid-sampling microdialysis. J Cereb Blood Flow Metab 2005; 25: 391–401.

Hossmann KA. Periinfarct depolarizations. [Review.] Cerebrovasc Brain Metab Rev 1996; 8: 195–208.

Leao AAP. Pial circulation and spreading depression of activity in the cerebral cortex. J Neurophysiol 1944a; 7: 391–6.

Leao AAP. Spreading depression of activity in cerebral cortex. J Neurophysiol 1944b; 7: 359–90.

Mayevsky A, Doron A, Manor T, Meilin S, Zarchin N, Ouaknine GE. Cortical spreading depression recorded from the human brain using a multiparametric monitoring system. Brain Res 1996; 740: 268–74.

Metea MR, Newman EA. Glial cells dilate and constrict blood vessels: a mechanism of neurovascular coupling. J Neurosci 2006; 26: 2862–70.

Mies G, Iijima T, Hossmann KA. Correlation between peri-infarct DC shifts and ischaemic neuronal damage in rat. Neuroreport 1993; 4: 709–11.

Narayan RK, Michel ME, Ansell B, Baethmann A, Biegon A, Bracken MB, et al. Clinical trials in head injury. [Review.] J Neurotrauma 2002; 19: 503–57.

Nedergaard M, Hansen AJ. Spreading depression is not associated with neuronal injury in the normal brain. Brain Res 1988; 449: 395–8.

Nimchinsky EA, Chuquet J, Hollender L. Spreading depression triggers astrocyte-mediated transient ischemia. Soc Neurosci Abstr 2006: 363.5.

Oberheim NA, Wang X, Goldman S, Nedergaard M. Astrocytic complexity distinguishes the human brain. Trends Neurosci 2006; 29: 547–53.

Ohta K, Graf R, Rosner G, Heiss WD. Profiles of cortical tissue depolarization in cat focal cerebral ischemia in relation to calcium ion homeostasis and nitric oxide production. J Cereb Blood Flow Metab 1997; 17: 1170–81.

Piper RD, Lambert GA, Duckworth JW, Piper RD, Lambert GA, Duckworth JW. Cortical blood flow changes during spreading depression in cats. Am J Physiol 1991; 261: H96–102.

Saito R, Graf R, Hubel K, Taguchi J, Rosner G, Fujita T, et al. Halothane, but not alpha-chloralose, blocks potassium-evoked cortical spreading depression in cats. Brain Res 1995; 699: 109–15.

Schroder ML, Muizelaar JP, Bullock MR, Salvant JB, Povlishock JT. Focal ischemia due to traumatic contusions documented by stable xenon-CT and ultrastructural studies. J Neurosurg 1995; 82: 966–71.

Shin HK, Dunn AK, Jones PB, Boas DA, Moskowitz MA, Ayata C. Vasoconstrictive neurovascular coupling during focal ischemic depolarizations. J Cereb Blood Flow Metab 2006; 26: 1018–30.

Siesjo BK. Pathophysiology and treatment of focal cerebral ischemia. Part II: mechanisms of damage and treatment. [Review.] J Neurosurg 1992; 77: 337–54.

Strong AJ, Bezzina EL, Anderson PJ, Boutelle MG, Hopwood SE, Dunn AK, et al. Evaluation of laser speckle flowmetry for imaging cortical perfusion in experimental stroke studies: quantitation of perfusion and detection of peri-infarct depolarisations. J Cerebral Blood Flow Metab 2006; 26: 645–53.

Strong AJ, Venables GS, Gibson G. The cortical ischaemic penumbra associated with occlusion of the middle cerebral artery in the cat: 1. Topography of changes in blood flow, potassium ion activity, and EEG. J Cereb Blood Flow Metab 1983; 3: 86–96.

Strong AJ, Harland SP, Meldrum BS, Whittington DJ. The use of in vivo fluorescence image sequences to indicate the occurrence and propagation of transient focal depolarizations in cerebral ischemia. J Cereb Blood Flow Metab 1996; 16: 367–77.

Strong AJ, Smith SE, Whittington DJ, Meldrum BS, Parsons AA, Krupinski J, et al. Factors influencing the frequency of fluorescence transients as markers of peri-infarct depolarizations in focal cerebral ischemia. Stroke 2000; 31: 214–22.

Strong AJ, Fabricius M, Boutelle MG, Hibbins SJ, Hopwood SE, Jones R, et al. Spreading and synchronous depressions of cortical activity in acutely injured human brain. Stroke 2002; 33: 2738–43.

Strong AJ, Hopwood SE, Boutelle MG, Parkin MC, Bezzina EL, Su Y, et al. Measuring dynamic changes in perfusion in the penumbra with high spatial and temporal resolution using laser speckle contrast imaging: comparison with indicator clearance. (Abstract) J Cereb Blood flow metab 2003: 23: 5300.

Takano K, Latour LL, Formato JE, Carano RA, Helmer KG, Hasegawa Y, et al. The role of spreading depression in focal ischemia evaluated by diffusion mapping. Ann Neurol 1996; 39: 308–18.

Takano T, Tian GF, Peng W, Lou N, Libionka W, Han X, et al. Astrocyte-mediated control of cerebral blood flow. [See Comment.] Nat Neurosci 2006; 9: 260–7.

Tower DB, Young OM. The activities of butyrylcholinesterase and carbonic anhydrase, the rate of anaerobic glycolysis, and the question of a constant density of glial cells in cerebral cortices of various mammalian species from mouse to whale. J Neurochem 1973; 20: 269–78.

Vajkoczy P, Roth H, Horn P, Lucke T, Thome C, Hubner U, et al. Continuous monitoring of regional cerebral blood flow: experimental and clinical validation of a novel thermal diffusion microprobe. J Neurosurg 2000; 93: 265–74.

Yanagisawa M, Kurihara H, Kimura S, Tomobe Y, Kobayashi M, Mitsui Y, et al. A novel potent vasoconstrictor peptide produced by vascular endothelial cells. [See Comment.] Nature 1988; 332: 411–5.